Thermoresponsive Shrinkage Triggered by Mesophase Transition in Liquid Crystalline Physical Hydrogels

Tatsuo Kaneko,[†] Kanji Yamaoka,[†] Yoshihito Osada,[†] and Jian Ping Gong*[,†,‡]

Division of Biological Sciences, Graduate School of Science, Hokkaido University, North 10, West 8, Kita-ku, Sapporo 060-0810, Japan, and Presto, JST

Received May 8, 2004

ABSTRACT: The hydrogel of poly(11-(4′-cyanobiphenyloxy)undecyl acrylate-*co*-acrylic acid), poly(11CBA-*co*-AA), which was comprised of the hydrophobic cross-linking junction zone with the liquid crystalline nature and the hydrated amorphous domain, showed a smectic mesophase transition at 40 °C in the body temperature range. X-ray diffraction study suggests the water transfer from the main chain domain of the liquid crystalline junction zone to the amorphous domain through the smectic transition. The oriented hydrogel fiber showed a drastic shrinkage through this transition, keeping the orientation. Moreover, the mesomorphic behavior of LCG depended on the aqueous milieu. Thus, the present LCG physically cross-linked by the mesomorphic junction could be considered to be an open system of new actuators controllable in the change in the aqueous milieu at ambient conditions.

Introduction

The soft actuators comprised of the polymers have widely attracted researchers' attention in the field of the material science for artificial muscles possibly applying to the robotics,[1−3] the space engineering,[1−3] and the medics,[4,5] since they are driven by an extremely low energy relative to the conventional actuator systems. The electronically driven systems using electroconductive[1,6−8] and ion-conductive polymers[9] have been focused in the technological fields shown above since the bending motion of the hydrogel−surfactant system was reported.[10] On the other hand, the magnetic field[11,12] and thermal energy[13,14] were used as other driving forces of the actuators. The actuator systems thermorsensitively driven in the body temperature range (ca. 34−42 °C) have a potential for the medical device actuating efficiently and safely. Especially, the actuating device triggered by the thermotropic phase transition like the living muscle systems may be useful as de Gennes theoretically showed a usefulness of polymeric networks with a liquid crystalline nature actuating through the phase transition.[15] Finkelmann[16] and others[17,18] have reported the efficient actuating behavior of the polymeric networks showing a liquid crystalline transition. Besides, Mather has recently reported the shape memory liquid crystalline elastomers actuating at ambient temperature.[19] As far as we know, however, there is no study on the liquid crystalline devices working at ambient temperature in the aqueous milieu which allows to transport the water-soluble materials into/out of the devices, although they are required for the medical use.

We have reported the liquid crystalline copolymer hydrogels[20−23] comprised of a hydrophobic monomer with a mesogenic moiety, 11-(4′-cyanobiphenyloxy)-undecyl acrylate (11CBA), and a hydrophilic monomer, acrylic acid (AA). The poly(11CBA-*co*-AA) showed the smectic A (SmA) phase in which side chains form bilayers aligning perpendicularly to the main chain axis.[20] These copolymers did not dissolve in water due to the hydrophobic nature of 11CBA but swelled to form hydrogels, keeping the liquid crystalline ordering (liquid crystalline gels; LCG).[21] LCG was the hydrated copolymers physically cross-linked by the hydrophobic junction zones with the liquid crystalline state where the mesogens can sensitively respond to environmental changes. When the water content exceeded at a certain value, LCG formed the smectic I (SmI) phase in which the side chains are tilted to the normal direction of main chain backbone and take a pseudohexagonal arrangement.[21] Such a structural change of LCG by water incorporation caused a discontinuous jump in Young's modulus.[23] When LCG in the SmI state is stretched, the necking occurs accompanied by a backward transition from SmI to SmA which also occurred at 40 °C in the body temperature range.[23] In this article, we reported the thermoresponsive actuating behavior of the oriented LCG investigating the thermotropic mesomorphic transition in detail and found a drastic shrinking in water in the body temperature range.

Experimental Section

Syntheses. 11-(4′-Cyanobiphenyloxy)undecyl acrylate (11CBA)[24,25] and poly(11-(4′-cyanobiphenyloxy)undecyl acrylate-*co*-acrylic acid), poly(11CBA-*co*-AA), were prepared by the procedures described in a previous paper.[20] The number- and weight-average molecular weight of poly(11CBA-*co*-AA) were 3000 and 3600, respectively, which are not high compared with those of common polymers but in the same order as those of poly(11CBA) in the literature.[24,25] The mole fraction of 11CBA unit, *F*, is defined as [11CBA]/([11CBA] + [AA]) and determined as 0.37 from ^{1}H NMR spectra of poly(11CBA-*co*-AA)s according to the method described in a previous paper.[20]

Preparation of Liquid Crystalline Hydrogel Fibers. Poly(11CBA-*co*-AA) (ca. 50 mg) melted in the SmA state at 120 °C to be the drop with a diameter of ca. 8 mm sticking to the glass plate. The SmA drop was drawn at a rate of 50 mm s^{-1} to yield the fiber 100 mm long and 0.8 mm thick in the SmA glass state. The fiber was immersed in the distilled water and swollen to yield the hydrogel fiber which was cut into the sample 40 mm long for the thermoresponse test.

Measurements. The optical microscopic observation was performed on a crossed-polarizing microscope (Olympus, BH-

[†] Hokkaido University. Current address of T.K.: Department of Molecular Chemistry, Graduate School of Engineering, Osaka University, 2-1 Yamadaoka, Suita, 565-0871, Japan.

[‡] Presto, JST.

* Corresponding author: Tel +81-11-706-2635; Fax +81-11-706-2635; e-mail gong@sci.hokudai.ac.jp.

10.1021/ma049096y CCC: $27.50
Published on Web 06/17/2004

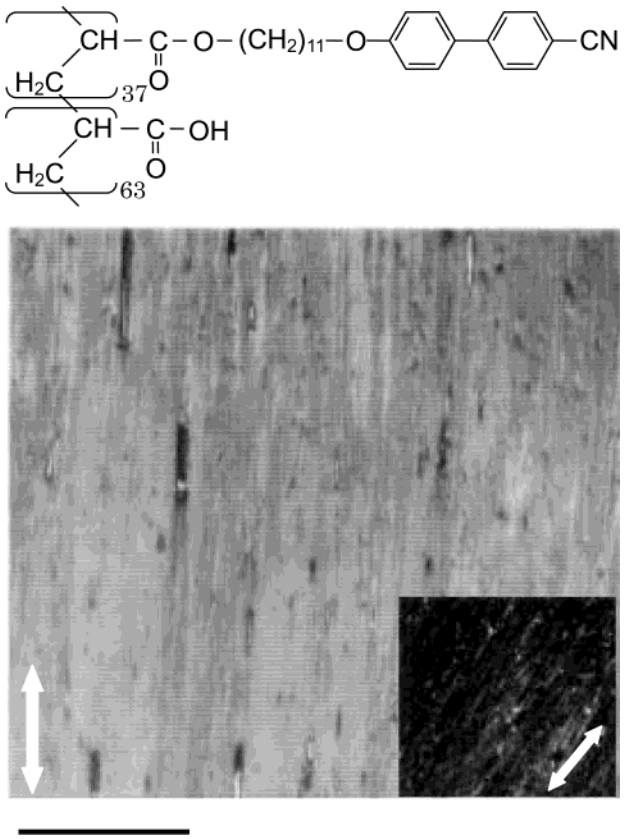

Figure 1. Crossed-polarizing microscopic photo of poly(11CBA-*co*-AA) hydrogel in the equilibrated water-swollen state when the fiber axis was located at an angle of 45° to either polarizers (taken at 25 °C). The inset shows the photo when the fiber axis was located parallelly to a polarizer. White arrows refer to the fiber direction. Scale bar: 10 μm. Molecular structure of poly(11CBA-*co*-AA) is shown at the top.

2). The sample was sandwiched between two glass plates in the water-swollen state. The texture was recorded on a digital camera. The thermotropic behavior was measured on a differential scanning calorimeter DSC (DSC22C, Seiko) at a scanning ratio of 5 °C min^{-1} from 0 to 100 °C. The water on the surface of the water-swollen samples (about 10 mg) was wiped off before hermetically sealed in aluminum pans. Transition enthalpy and entropy were calculated with respect to 11CBA units. Wide-angle X-ray diffraction (WAXD) patterns were taken with a flat-plate camera mounted to a Shimazu X-ray generator XD-610 emitting Ni-filtered Cu Kα radiation at 40 kV and 40 mA in transmission geometry. The distance from the sample to the film was determined by calibration with silicone powder. Small-angle X-ray diffraction (SAXD) patterns were recorded on a Rigaku X-ray diffractometer (RINT-2000) at 40 kV and 200 mA in transmission geometry. A 2θ scanning speed of 1° min^{-1} with a sampling interval of 0.01° was used. The degree of swelling, q, was defined as the weight ratio of a swollen gel to the dried one.

Results and Discussion

The LCG fiber prepared by immersing the poly(11CBA-*co*-AA) one (Figure 1) into water was observed under the crossed-polarizing microscope. The field of view was very bright, and many striped lines were observed along the longitudinal direction of the fiber which was set with forming an angle of about 45° to both polarizers (Figure 1) while the field became dark when the fiber direction was rotated to be parallel to either polarizer (inset). This birefringence behavior was observed in the whole fiber, demonstrating the macroscopic orientation of LCG. Our previous report proposed

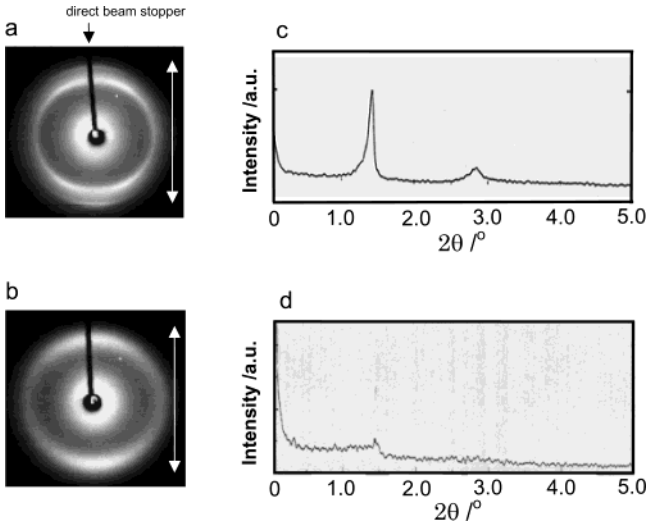

Figure 2. X-ray diffraction patterns of poly(11CBA-*co*-AA) hydrogels. Wide-angle X-ray diffraction (WAXD) images taken in the pure water (a) at 25 °C and (b) at 60 °C. White arrows refer to the fiber axis. Small-angle X-ray diffraction (SAXD) diagrams taken in the pure water (c) at 25 °C and (d) at 60 °C.

that LCG was comprised of the hydrophobic cross-linking junction forming the liquid crystalline structure and the hydrophilic amorphous domain.[21] The present birefringence behavior suggests that the amorphous domain was oriented along the fiber direction according to the orientation of the liquid crystalline domain.

The WAXD image showed the pattern with six diffraction spots characteristic of the smectic I (SmI) structure (Figure 2a), and the SAXD diagram showed two distinct diffraction peaks at $2\theta = 1.41°$ and 2.82° (θ = diffraction angle), corresponding to spacings of 6.27 and 3.13 nm, confirming the bilayer structure with a thickness of 6.27 nm (Figure 2c) as described in a previous paper.[21] The SmI structure was schematically illustrated in Figure 3a where the hydrated acrylic acid domain and the hydrophobic mesogenic domain were alternatively laminated to form the bilayer structure. The DSC thermodiagram on heating showed an endothermic peak at around 40 °C with a latent heat (enthalpy change) of 6.4 kJ mol^{-1} corresponding to the entropy change of 2.0 kJ mol^{-1} K^{-1} (Figure 4a). Since the changes in enthalpy and entropy were in the same order of the values which is a general feature of liquid crystalline transition for the mesogenic polymers, the DSC peak may be related to the liquid crystalline phase transition.[26]

The WAXD image of LCG fiber swollen in water at 70 °C for 3 h was taken at the same temperature (Figure 2b), and the mesomorphic structure was analyzed in order to confirm the mesophase transition. The WAXD pattern characteristic of the SmI structure disappeared at 70 °C; instead, two board diffraction spots appeared on the meridian line, indicating the random arrangement of side chains perpendicular to the fiber axis. The SAXD pattern taken at 70 °C showed a small peak at $2\theta = 1.44°$ (Figure 2d), corresponding to the 6.14 nm which is slightly shorter than the bilayer spacing at 25 °C. As a result, the hydrogel formed the SmA structure at 70 °C and the endotherm appearing in the DSC thermogram can be assigned to the SmI−SmA transition.

The mesomorphic transformation is schematically illustrated in Figure 3. In LCG fiber, the hydrated

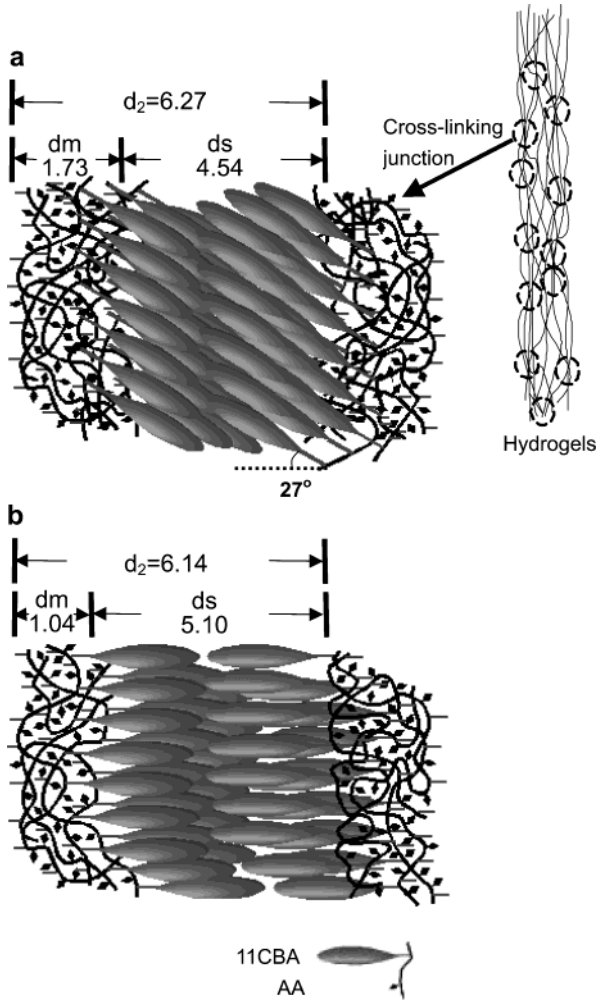

Figure 3. Schematic illustration of the poly(11CBA-*co*-AA) hydrogel fiber. The network structure is shown at the top right, where the portion circled by the dotted line refers to the cross-linking junction zone, and the amorphous domain was oriented along the fiber axis. The mesomorphic structure of the cross-linking junction at 25 and 60 °C is illustrated in (a**)** and (b**)**. The unit of *d* values is nm.

amorphous domain and the hydrophobic liquid crystalline junction zone were both oriented as shown in the illustration at the upper right of Figure 3. The expanded view of the cross-linking junction circled by the dotted line is illustrated in parts a and b of Figure 3, showing the structures of SmI (25 °C) and SmA (70 °C), respectively. The bilayer spacing, d_2, showed a slight decrease from 6.27 to 6.14 nm in the SmI−SmA transition. However, the thickness of the side chain domain, d_s, in the SmI state could be calculated as 4.54 nm since the side chain, twice the length of which was calculated as 2.55 nm using a CPK model based on the assumption of the fully extended conformation, tilted at an angle of about 27° to the normal line of the bilayer. On the other hand, d_s was calculated as 5.10 nm in the SmA state. The transformation from the SmI−SmA structure gave an increase in d_s. If the thickness of the main chain domain, d_m, is calculated as the equation $d_m = d_2 - d_s$, it decreases from 1.73 to 1.04 nm through the SmI−SmA transition, which shows a dehydration of the main chain domain. The increased hydrophobicity of the side chains domain by heating may induce such dehydration. Contrarily, the water content of the amorphous domain of LCG should be enhanced by heating. Since the swelling degree *q* of the hydrogel at 70 °C was $q = 1.19$, almost equal to the value of $q = 1.18$ at 25 °C, the water may transfer from the main chain domain of the smectic bilayer into the amorphous domain by the SmI−SmA transition inside the hydrogel. The transfer of the water may affect the orientation of the hydrogel.

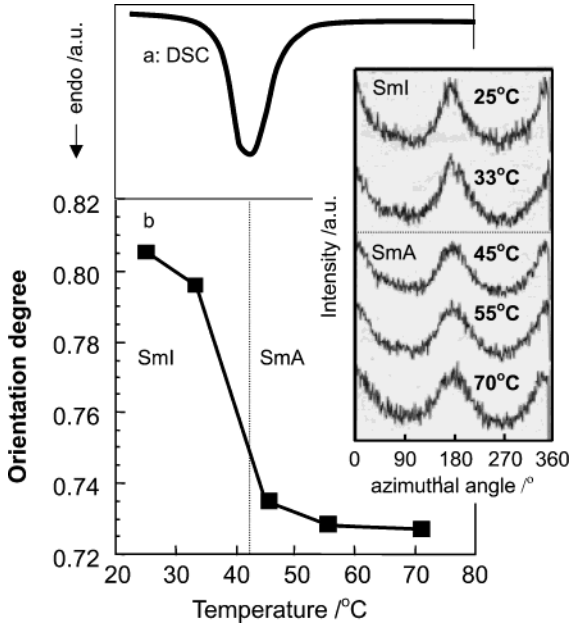

Figure 4. Temperature dependence of the WAXD azimutal scanning for the poly(11CBA-*co*-AA) hydrogel fiber. The heating thermogram measured by differential scanning calorimetry (DSC) is shown in (a**)**. Plots of orientation degree against the temperature are shown in (b). Orientation degrees were estimated from the azimuthal scanning diagrams in SmI and SmA state in terms of $2\theta = 3.8°$ and 4.5°, respectively (the inset where the shadow of the direct beam stopper of Figure 2 was located at 360°).

The effects of the SmI−SmA transition on the orientation of LCG were investigated. The azimuthal scanning of the WAXD patterns of SmI and SmA structures was made around the diffractions at $2\theta = 3.8°$ and 4.5°, respectively. The inset of Figure 4 shows the azimuthal scanning diagrams, giving the distinct peaks around 0° (360°: the location of the direct beam stopper) and 180° corresponding to the meridian line. From these diagrams, the orientation degree was estimated using the equation $(360 - \beta)/360$, where β refers to the summation of the azimuthal angles of the full width at the half-maximum of diffraction arcs[27] and plotted against temperature (Figure 4b). The orientation degree abruptly dropped at around 40 °C, which corresponds to the SmI−SmA transition. Although the better hydrated polymer chains cross-linked by the lower ordered domain in the SmA phase gave a lower orientation degree than those in the SmI phase, it is notable that the SmA junction still has a capability to keep the orientation of the polymer chains. The smectic transition induced a small decrease in the orientation degree, which should give the shrinkage of LCG fiber.

The shrinking behavior of the oriented LCG through this transition was investigated. One end of the oriented LCG fiber 40 mm long and 1 mm wide was fixed on the glass substrate equipped with the hot stage which was heated at a rate of 5 °C min^{-1} (another end was free). When the hot stage exceeded 40 °C, the gel shrank as shown in Figure 5. The temperature dependence of the fiber length is shown in Figure 5. The percentage of the fiber length to the initial length began to decrease at

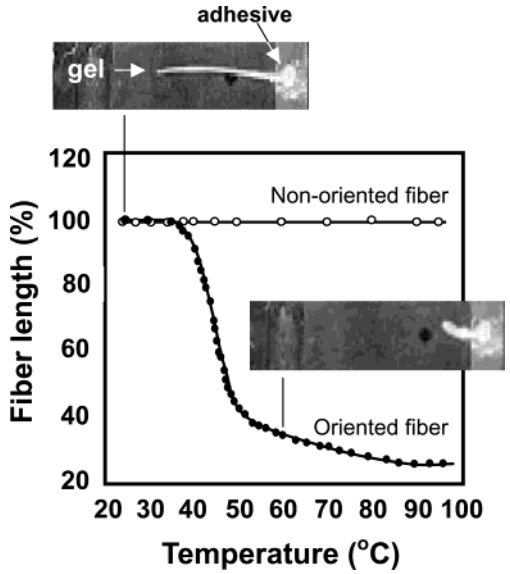

Figure 5. Temperature dependence of the percent of the fiber length to the original length of the poly(11CBA-*co*-AA) hydrogel fiber oriented and nonoriented. The pictures of the poly(11XBA-*co*-AA) hydrogel fiber whose right end is fixed on the glass plate by adhesive set with the temperature-controllable hot stage are shown together.

around 40 °C, which corresponded to the endothermic temperature measured by DSC and showed a drastic drop down to 25% within 10 min at 80 °C. On the other hand, the percentage of the fiber width to the initial width increased up to about 200% at 80 °C, indicating the maintenance of the initial volume during the transition. The shrinking time was reduced to about 5 s if the LCG was put into the hot water at 90 °C, indicating that the heat diffusion was a significant factor to control the shrinking rate. On the other hand, the nonoriented hydrogel fiber prepared by water immersion of the sample spun from the isotropic state in the dry condition showed no change in the length. This finding showed that the shrinking behavior was related to the structural orientation of LCG. However, the shrinking ratio of LCG is so big that we cannot explain it only from the small decrease in the orientation degree. Another reason for the big shrinkage may be entropic effects of the stretched amorphous domain relaxing through the water content increase in the amorphous domain and molecular mobility increase in the cross-linking junction zone by the SmI−SmA structural disordering. In this case, it can be considered that the present LCG drives as a result of the shape memory effects. Thus, the actuator shrinking in water at body temperature could be developed using LCG.

Moreover, the mesomorphic behavior of LCG depended on the aqueous milieu. When LCG was immersed in water of pH = 3.4, 4.6, 8.0, and 9.5 whose ionic strength was kept to be 0.01 M by adding NaCl, it showed different q values of 1.13, 1.15, 2.78, and 3.12, respectively, which were measured at 25 °C. X-ray studies confirmed that LCG showed SmI structure at pH = 3.4 and 4.6 while it showed no specific structure at pH = 8.0 and 9.5 (at 25 °C). Besides, LCG showed an increase in the bilayer spacing from 6.12 to 6.22 nm with an increase in pH from 3.4 to 4.6. Since the ionization degree of poly(acrylic acid) remarkably increased up to 80% with an increase in pH up to 8 according to the previous study,[28] the change in q and bilayer spacing may be due to the ionization of AA units. These results demonstrated that hydroxyl anions freely imported from the water into LCG. We expect that the present LCG physically cross-linked by the LC junction could be considered to be an open system of new actuators controllable in the change in the aqueous milieu at ambient conditions.

Acknowledgment. This research was financially supported by the Grant-in-Aid for Creative Scientific Research from the MEXT, Japan, and by a Grant-in-Aid for The Sumitomo Foundation and Industrial Technology Research Grant Program in 03A44014c from New Energy and Industrial Technology Development Organization (NEDO) of Japan.

References and Notes

(1) Bar-Cohen, Y. *J. Spacecr. Rockets* **2002**, *39*, 822.
(2) Bar-Cohen, Y. *Ind. Robot* **2003**, *30*, 331.
(3) Shahinpoor, M.; Bar-Cohen, Y.; Simpson, J. O.; Smith, J. *Smart Mater. Struct.* **1998**, *7*, R15.
(4) Smela, E. *Adv. Mater.* **2003**, *15*, 481.
(5) Lehmann, W.; Skupin, H.; Tolksdorf, C.; Gebhard, E.; Zentel, R.; Kruger, P.; Losche, M.; Kremer, F. *Nature (London)* **2001**, *410*, 447.
(6) Lu, W.; Fadeev, A. G.; Qi, B. H.; Smela, E.; Mattes, B. R.; Ding, J.; Spinks, G. M.; Mazurkiewicz, J.; Zhou, D. Z.; Wallace, G. G.; MacFarlane, D. R.; Forsyth, S. A.; Forsyth, M. *Science* **2002**, *297*, 983.
(7) Bay, L.; West, K.; Sommer-Larsen, P.; Skaarup, S.; Benslimane, M. *Adv. Mater.* **2003**, *15*, 310.
(8) Baughman, R. H.; Cui, C. X.; Zakhidov, A. A.; Iqbal, Z.; Barisci, J. N.; Spinks, G. M.; Wallace, G. G.; Mazzoldi, A.; De Rossi, D.; Rinzler, A. G.; Jaschinski, O.; Roth, S.; Kertesz, M. *Science* **1999**, *284*, 1340.
(9) Shahinpoor, M. *Electrochim. Acta* **2003**, *48*, 2343.
(10) Osada, Y.; Okuzaki, H.; Hori, H. *Nature (London)* **1992**, *355*, 242.
(11) Zrinyi, M. *Colloid Polym. Sci.* **2000**, *278*, 98.
(12) Juliac, E.; Mitsumata, T.; Taniguchi, T.; Iwakura, K.; Koyama, K. *J. Phys. Chem. B* **2003**, *107*, 5426.
(13) Osada, Y.; Matsuda, A. *Nature (London)* **1995**, *376*, 219.
(14) Tajbakhsh, A. R.; Terentjev, E. M. *Eur. Phys. J. E* **2001**, *6*, 181.
(15) de Gennes, P.; Hebert, M.; Kant, R. *Macromol. Symp.* **1997**, *113*, 39.
(16) Camacho-Lopez, M.; Finkelmann, H.; Palffy-Muhoray, P.; Shelley, M. *Nature Mater.* **2004**, *3*, 307.
(17) Li, M. H.; Keller, P.; Albouy, P. A. *Macromolecules* **2003**, *36*, 2284.
(18) Thomsen, D. L.; Keller, P.; Naciri, J.; Pink, R.; Jeon, H.; Shenoy, D.; Ratna, B. R. *Macromolecules* **2001**, *34*, 5868.
(19) Rousseau, I. A.; Mather, P. T. *J. Am. Chem. Soc.* **2003**, *125*, 15300.
(20) Kaneko, T.; Yamaoka, K.; Gong, J. P.; Osada, Y. *Macromolecules* **2000**, *33*, 412.
(21) Kaneko, T.; Yamaoka, K.; Gong, J. P.; Osada, Y. *Macromolecules* **2000**, *33*, 4422.
(22) Yamaoka, K.; Kaneko, T.; Gong, J. P.; Osada, Y. *Macromolecules* **2001**, *34*, 1470.
(23) Yamaoka, K.; Kaneko, T.; Gong, J. P.; Osada, Y. *Langmuir* **2003**, *19*, 8134.
(24) Shibaev, V. P.; Kostromin, S. G.; Plate, N. A. *Eur. Polym. J.* **1982**, *18*, 651.
(25) Kostromin, S. G.; Sinitzyn, V. V.; Talroze, R. V.; Shibaev, V. P.; Plate, N. A. *Makromol. Chem., Rapid Commun.* **1982**, *3*, 809.
(26) Demus, D.; Goodby, J.; Gray, G. W.; Spiess, H.-W.; Vill, V. *Handbook of Liquid Crystals;* Wiley-VCH: Weinheim, 1998.
(27) Kakudo, M.; Kasai, N. *X-ray Diffraction by Polymers*; Kodansha: Tokyo, 1972.
(28) Matsuda, A.; Katayama, Y.; Kaneko, T.; Gong, J. P.; Osada, Y. *J. Mol. Struct.* **2000**, *554*, 91.

MA049096Y